J|A|C|S COMMUNICATIONS

Published on Web 10/29/2010

Ag_9 Quantum Cluster through a Solid-State Route

Thumu Udaya B. Rao, Bodappa Nataraju, and Thalappil Pradeep*

DST Unit on Nanoscience (DST UNS), Department of Chemistry and Sophisticated Analytical Instrument Facility, Indian Institute of Technology Madras, Chennai 600 036, India

Received June 23, 2010; E-mail: pradeep@iitm.ac.in

Abstract: A silver cluster having the composition $Ag_9(H_2MSA)_7$ (H_2MSA = mercaptosuccinic acid) was synthesized in macroscopic quantities using a solid-state route. The clusters were purified by PAGE and characterized by UV−vis, FTIR, luminescence, and NMR spectroscopy, TEM, XPS, XRD, TG, SEM/EDAX, elemental analysis, and ESI MS. The solid-state route provides nearly pure Ag_9 clusters, and nanoparticle contamination was insignificant for routine studies. Formation of various clusters was observed by modifying the conditions. The effect of ligands on the synthesis was checked. The cluster decomposed slowly in water, and the decomposition followed first-order kinetics. However, it could be stabilized in solvent mixtures and in the solid state. Such materials may be important in cluster research because of their characteristic absorption profiles, which are similar to those of Au_{25} and Au_{38}. The cluster showed luminescence with a quantum yield of 8×10^{-3} at 5 °C.

Noble-metal quantum clusters (QCs) showing confinement in their absorption profiles are fascinating materials that are the subject of intense research today.[1] Breakage of continuous-energy bands of the metallic nanoparticles into discrete energy levels leads to unusual properties such as steplike behavior in the absorption profile,[1] orders of magnitude enhancement in luminescence in comparison with metal nanoparticles,[1g,k] and unusual intrinsic magnetism.[2] Several of their applications in areas such as catalysis,[3] medicine,[4] nanoelectronics,[5] and nanophotonics[6] have been demonstrated. QCs of gold have been particularly well-studied because of their extraordinary chemical stability as well as rich variety in optical properties. However, commensurate expansion has not happened in the area of silver QCs. There have been several examples of template-assisted syntheses of water-soluble, highly luminescent Ag_n ($n = 2-8$) clusters.[7] However, there have been only limited efforts in the case of monolayer-protected analogues, which include the synthesis of thiolate-protected silver QCs.[8−10] The methods used for the synthesis of gold QCs are not totally successful in the synthesis of their silver analogues, and alterations have been done to prepare arylthiol-,[8] dithiol-,[9] and chiral thiol-protected[10] clusters. None of the methods can produce gram-scale quantities of the materials for subsequent studies, except for the one reported by Jin and co-workers.[9]

Here we report the direct synthesis by a solid-state route of a silver QC consisting of a nine-atom core protected with mercaptosuccinic acid (H_2MSA) that exhibits well-defined transitions in its absorption profile. The material was synthesized in gram quantities by minimizing the diffusion of the reactants in the growth step, as they are mixed in the solid state. This kind of cluster produced by the solid-state route is different from those synthesized previously.[8−10] This new synthetic approach may make possible the synthesis of clusters of other elements, such as Cu, Au, Pt, Pd, and so on.

The process for synthesizing the cluster was simple and involved three steps (see section S1 in the Supporting Information for details). First, a mixture of $AgNO_3$ (**1**) and H_2MSA (**2**) in a 1:5 molar ratio was ground in the solid state until a change of color from colorless to orange occurred. This showed that a reaction between **1** and **2** occurred at the interface between the particles as a result of the strong affinity of sulfur for noble metal ions, and the likely product is silver thiolate. Second, sodium borohydride (5-fold molar excess with respect to **1**) in solid form was added, and the mixture was ground, resulting in the formation of a brownish black powder that showed a strong affinity for water. At this point, the compounds were mixed well, and the particle growth was controlled because of the lack of protic solvent, which facilitates fast reduction to form metallic particles. A cluster solution was formed with a strong effervescence due to the release of hydrogen as 15 mL of water was added over a period of 1 min. These clusters were precipitated by the addition of excess ethanol. After the clusters were washed with the alcohol, a fine reddish-brown powder was obtained by

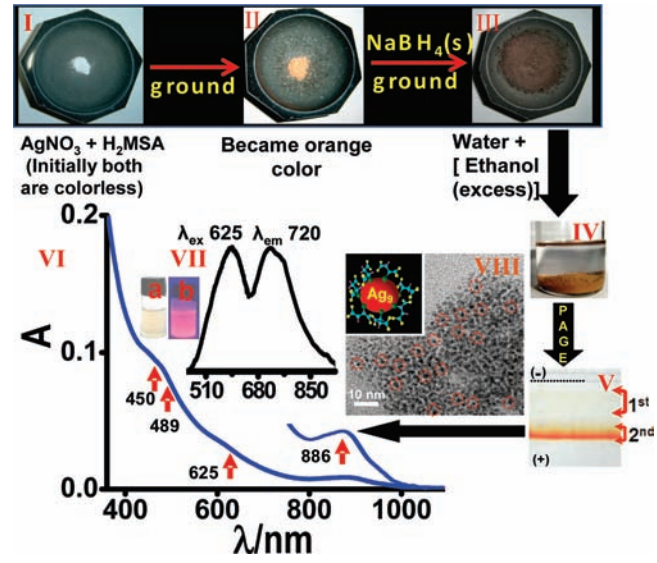

Figure 1. (I−IV) Photographs representing the changes during the cluster synthesis. Photograph I shows the initial mixture of **1** and **2**, both of which are colorless solids. Grinding for 10 min led to the formation of an orange-colored powder, likely to be due to the formation of a silver(I)−H_2MSA complex (photograph II). To that solid mixture, $NaBH_4$ was added and mixed, after which the color changed from orange to reddish-brown (photograph III). Distilled water (15 mL) was slowly added to the above powder over 1 min. The clusters formed were precipitated immediately by the addition of ethanol (photograph IV). (V) PAGE of the crude mixture showed the presence of two bands in visible light. (VI) UV−vis profile of the pure cluster, showing dominant steplike behavior. Arrows indicate the well-defined optical features of the cluster. (VII) Luminescence spectrum of the cluster in 1:1 water/methanol at 5 °C. Insets (a) and (b) show a 4 mg/mL cluster solution in water/methanol under white and UV light, respectively, at 5 °C. (VIII). TEM image of the PAGE-separated clusters. The inset shows a schematic of the QC prepared.

10.1021/ja105495n

solvent evaporation. Slow addition of water gave a good amount of clusters in comparison with fast addition (section S2). It was essential to use all of the chemicals in the solid form to obtain the desired results (section S3). Several systematic control experiments were done to improve the yield of clusters and suppress the formation of metallic nanoparticles (section S4). Photographs of the steps used are shown in Figure 1I−IV.

Polyacrylamide gel electrophoresis (PAGE) of the crude cluster showed two bands: the first was pale-yellow and the second bright-red in visible light (Figure 1V). The first band was composed of metallic nanoparticles, as indicated by the surface plasmon feature at 400 nm. The second band gave the same distinct absorption features as the crude cluster (section S5), demonstrating that the clusters were nearly pure in the as-synthesized form and were largely free of plasmonic NPs. The PAGE-separated cluster showed a strong quantum size effect similar to those observed in calculations,[11] such as a near-IR absorption peak at 886 nm (1.4 eV) and features at 625 (1.98), 450 (2.76), 479 (2.60), and 315 (3.95) nm (eV) in the UV-vis spectrum (Figure 1VI). The materials before and after PAGE showed luminescence with excitation and emission maxima at 625 and 720 nm, respectively (Figure 1VII). The quantum yield (QY) was 8×10^{-3} in 1:1 (v/v) water/MeOH at 5 °C. The observed QY is comparable to those of several QCs.[1c,8b,10c] Spectral decomposition to obtain a better estimate of absorbance at 625 nm may result in a higher QY. There was no observable shift in the peak position after PAGE, but there was a slight increase in the intensity (section S6). The Raman spectrum of the pure cluster powder showed a strong luminescence background upon excitation at 532 nm (section S7), confirming the existence of smaller clusters. The cluster appeared as tiny dots in the transmission electron microscopy (TEM) image (Figure 1VIII), which upon longer electron beam irradiation aggregated to form nanoparticles (section S8). Such electron-beam-induced aggregation is known in QCs.[10d]

The cluster degraded slowly in an aqueous medium. The peak intensities of the cluster decreased with time without changing position, and finally, a featureless spectrum was seen (section S9). This type of decomposition in an aqueous medium is known from previous reports of PAGE-separated clusters[10a,b] and those obtained from cyclic oxidative reduction conditions.[10c] We attempted to stabilize these clusters upon consideration of several points: (1) Decomposition of QCs in water was highly concentration-dependent. The rate of decomposition followed first-order kinetics, as studied by UV−vis spectroscopy (section S10). The rate constants calculated were 3.02×10^{-4} and 1.3×10^{-3} s^{-1} for 5 and 2 mg/3 mL initial concentrations, respectively. (2) The stability of the cluster solution in water was greater at higher pH than at lower pH. Thus, the addition of a less polar solvent such as methanol, acetonitrile, or ethanol and maintaining pH at 8 stabilized the cluster, and it remained intact for several months under laboratory conditions without any change in absorption-peak positions (section S11). Cluster decomposition produced thiolates with characteristic peaks in electrospray ionization mass spectrometry (ESI MS) (section S12).

ESI MS was used to understand the composition of the cluster. Several of the monloayer-protected gold clusters produce multiply charged species upon soft ionization. Cluster MS is especially useful in the case of silver, as its specific isotope pattern allows precise identification of the composition and charge state of the ion.[12,10d] Negative-ion ESI MS measurements on the PAGE-separated clusters in 1:1 water/methanol (Figure 2) showed characteristic signatures due to silver clusters. These features were also seen in the mass spectrum of the crude product. From a detailed analysis of the mass spectrum, a chemical composition of $Ag_9(H_2MSA)_7$ can be assigned to the molecular species obtained in this synthesis. The experimentally observed isotope distribution matched perfectly with the calculated pattern. For example, the peaks due to $Ag_9(H_2MSA)_6(MSA)^{2-}$ (*m*/*z* 1007) and $NaAg_9(H_2MSA)_5(HMSA)(MSA)^{2-}$ (*m*/*z* 1018) were in good agreement with the calculated values (1006.4 and 1017.4, respectively). It should be noted that H_2MSA is a dicarboxylic acid (giving the MSA^{2-} dianion after complete ionization), and therefore, it can exist in the cluster as either negatively charged species or in the form of sodium adducts, giving clusters with the formula $\{Ag_9(MSA)_7H_{14-(n+2)}Na_n\}^{2-}$ (n = 0, 1, ..., 12). For example, the dianion on Ag_9 with MSA protection can result in 13 cluster peaks, ranging from $Ag_9(H_2MSA)_6(MSA)^{2-}$ to $Na_{12}[Ag_9(MSA)_7]^{2-}$ (section S13). Along with these peaks, several singly charged species [e.g., $Ag_4(MSA)_3^-$, $Ag_3(MSA)_3^-$, etc.] and their sodium adducts were also observed. These latter peaks are due to silver−thiolate complexes resulting from cluster dissociation upon ionization. These are colored blue in the expanded view of the mass spectrum. A separation of *m*/*z* 22 can be understood in terms of the loss of the proton along with the addition of Na. MALDI MS, in contrast, gave a series of silver sulfide species with characteristic spacing. This is a result of C−S bond cleavage upon 337 nm laser impact (section S14).[1g,k]

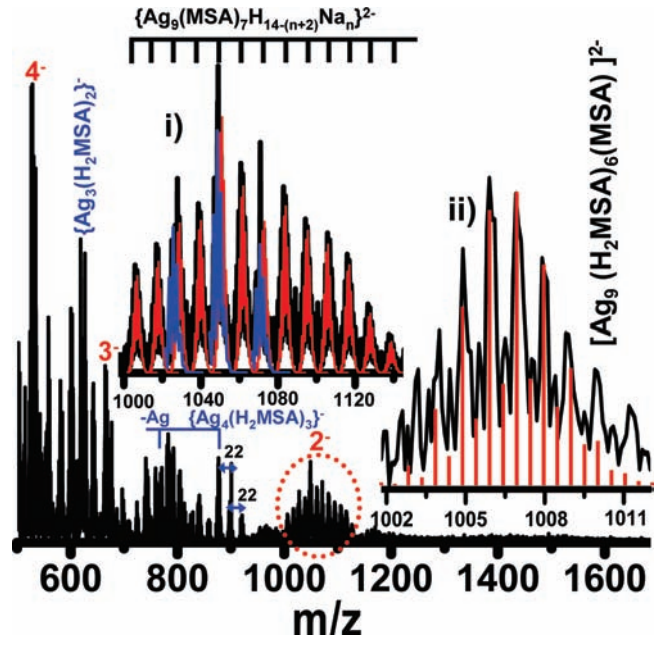

Figure 2. ESI MS spectrum of PAGE-separated $Ag_9(H_2MSA)_7$ clusters in the negative mode in the region *m*/*z* 500−1700. Inset (i) shows an expanded spectrum of the cluster ion $\{Ag_9(MSA)_7H_{14-(n+2)}Na_n\}^{2-}$ overlapped with peaks due to $[Ag_4(H_2MSA)_3HMSA]^-$ and its sodium adducts, which are shown in blue. Inset (ii) shows a comparison of the expected and observed peaks for $[Ag_9(H_2MSA)_6(MSA)]^{2-}$.

The molecular formula and nature of the monolayer binding are supported by X-ray photoelectron spectroscopy (XPS) (section S15), FT-IR spectroscopy (section S16), and energy-dispersive X-ray analysis (EDAX) (section S17). The Ag/S atomic ratios measured using EDAX and XPS are 1:0.75, and 1:0.76, respectively, in agreement with the expected ratio (1:0.77). The XPS survey spectrum shows all of the expected elements. The Ag 3d peak is close to an Ag(0) value. The S $2p_{3/2}$ peak is thiolate-like with an observed value of 161.8 eV (section S15). This is in agreement with the IR spectrum, which suggests the loss of thiolate proton upon cluster formation (section S16).

Thermogravimetric (TG) analysis of $Ag_9(H_2MSA)_7$ under an inert atmosphere (N_2) displayed a two-step mass loss (first and second steps are ~23 and ~28% for three and four thiolates, respectively) in the 190−500 °C window (section S18). The observed mass loss of 51.3% matches the organic weight fraction of 51.9% expected for $Ag_9(H_2MSA)_7$. Asymmetry in ligand binding is evident from the TG data. In view of the presence of water, elemental analysis is prone to error, and the CHNS analysis data given in section S19 show an enhanced H percentage due to water. However, the C and S percentages are close to the expected values. The formation of small clusters in the reaction was confirmed by the X-ray diffraction (XRD) pattern of the crude cluster, which showed a broad peak centered around $2\theta \approx 38°$, and the characteristic peaks exhibited by metallic Ag@H_2MSA nanoparticles were absent (section S20). Several silver QCs show only the broad feature.[7c,10d,e] A broad peak at $2\theta \approx 35°$ was observed in the case of Au_{20}.[1d]

The ^{1}H and ^{13}C NMR spectra of H_2MSA and $Ag_9(MSA)_7$ clusters were measured in D_2O and are shown in Figure 3. The spectra of Ag(I)MSA (sodium salt of thiolate) were also measured for comparison. The carbon atoms and hydrogens attached to them are labeled with the letters b and a, respectively (Figure 3). Two strong multiplets at 2.8 and 3.7 ppm in the ^{1}H spectrum are apparently from these CH_2 and CH, respectively. These multiplets are broadened in the QC. The CH protons are shifted downfield because of the proximity to the silver core. The other set of protons (CH_2) follows similar shift as in the case of Ag(I)MSA but are broadened. The ^{13}C NMR spectrum of free H_2MSA (Ag(I)MSA) in D_2O shows four different carbon resonances due to two carboxyl carbons at 176.6 and 174.7 (180.7 and 178.7) ppm and methylene and methyne carbons at ~35.8 and 39.3 (41.2 and 44.5) ppm, respectively. For Ag(I)MSA, all of the carbon signals of the ligands are shifted downfield. However, a complex spectrum with significant broadening was observed in the case of $Ag_9(MSA)_7$. The methyne and methylene carbons show two distinct chemical environments as in $Au_{25}L_{18}$,[1b,c,l] giving four features and supporting the TG data. The carboxylate carbons are too broad to allow further analysis. On the basis of all of the measurements discussed above, we excluded the possibility of silver sulfide or its clusters in the reaction product. $Ag_9(H_2MSA)_7$ is a two-electron system and is therefore stable according to the spherical jellium model.[11]

To check the effect of solvent polarity on the synthesis, various solvents were used. The major peaks in the UV−vis spectra were observed at 530, 480, 490, and 485 nm for dichloromethane, methanol, ethanol, and dimethylformamide, respectively. These cluster samples run on agarose (2%) showed the presence of a single band (section S21). Various ligands, including glutathione, cysteine, and 2,3-dimercaptosuccinic acid, were tried instead of H_2MSA in the synthesis. In the case of glutathione, the data support the formation of a new cluster whose absorption profiles have a major peak at ~500 nm and shoulders at 350, 550, and 630 nm, all of which are similar to those of Ag_7 reported by Jin and co-workers[9] (section S22). The major peak at 500 nm was also seen in the case of cysteine. However, these absorption profiles are highly sensitive to atmospheric oxygen, and therefore, to stabilize the clusters, a N_2 atmosphere is required.

In summary, an Ag_9 cluster exhibiting quantum confinement was synthesized by a solid-state route. The clusters were purified by PAGE and characterized by UV−vis, FTIR, luminescence, and NMR spectroscopy, TEM, XPS, XRD, TG, SEM/EDAX, elemental analysis, and ESI MS. These clusters are highly stable in the solid state under an inert atmosphere or preserved in ethanol. The clusters are also stable in solvent mixtures with water as one of the components. Our results provide essential data for further experimental and theoretical studies of the geometric and electronic structures as well as photophysical properties of Ag_9.

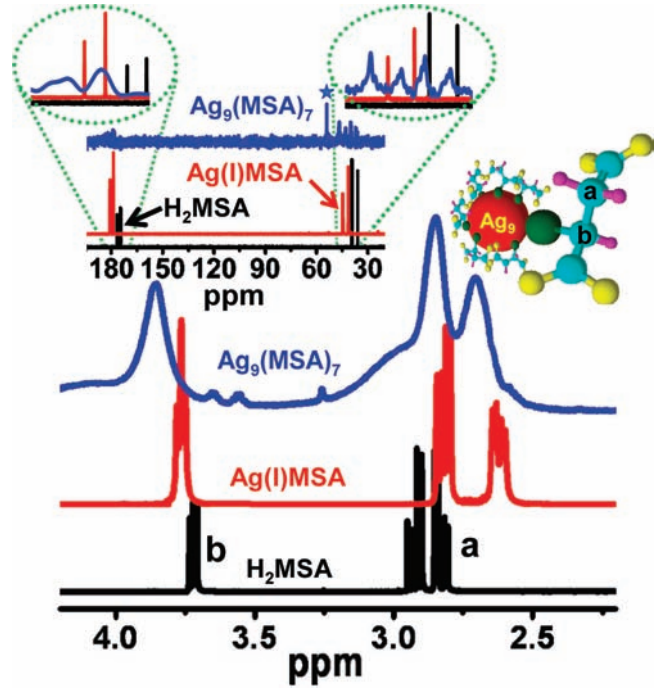

Figure 3. ^{1}H NMR spectrum of the cluster extracted in D_2O after gel electrophoresis, along with the spectrum of H_2MSA. The inset shows the ^{13}C NMR spectra of H_2MSA, Ag(I)MSA, and $Ag_9(MSA)_7$. The asterisk indicates the peak of the CH_2 carbon of residual ethanol (from purification). Portions of the ^{13}C spectrum of $Ag_9(MSA)_7$ are expanded.

Acknowledgment. We thank the Department of Science and Technology of the Government of India for constantly supporting our research program on nanomaterials.

Supporting Information Available: Details of experimental procedures and characterization using UV−vis, control measurements, luminescence, TEM, ESI MS, MALDI MS, XPS, FT-IR, TG, XRD, and CHNS analysis of $Ag_9(H_2MSA)_7$ clusters. This material is available free of charge via the Internet at http://pubs.acs.org.

References

(1) (a) Jadzinsky, P. D.; Calero, G.; Ackerson, C. J.; Bushnell, D. A.; Kornberg, R. D. *Science* **2007**, *318*, 430. (b) Heaven, M. W.; Dass, A.; White, P. S.; Holt, K. M.; Murray, R. W. *J. Am. Chem. Soc.* **2008**, *130*, 3754. (c) Jin, R. *Nanoscale* **2010**, *2*, 343, and references cited therein. (d) Zhu, M.; Qian, H.; Jin, R. *J. Am. Chem. Soc.* **2009**, *131*, 7220. (e) Chaki, N. K.; Negishi, Y.; Tsunoyama, H.; Shichibu, Y.; Tsukuda, T. *J. Am. Chem. Soc.* **2008**, *130*, 8608. (f) Zhu, M.; Lanni, E.; Garg, N. M.; Bier, E.; Jin, R. *J. Am. Chem. Soc.* **2008**, *130*, 1138. (g) Habeeb Muhammed, M. A.; Verma, P. K.; Pal, S. K.; ArunKumar, R. C.; Paul, S.; Omkumar, R. V.; Pradeep, T. *Chem.—Eur. J.* **2009**, *15*, 10110. (h) Toikkanen, O.; Ruiz, V.; Ronnholm, G.; Kalkkinen, N.; Liljeroth, P.; Quinn, B. M. *J. Am. Chem. Soc.* **2008**, *130*, 11049. (i) Qian, H.; Zhu, Y.; Jin, R. *J. Am. Chem. Soc.* **2010**, *132*, 4583. (j) Dass, A. *J. Am. Chem. Soc.* **2009**, *131*, 11666. (k) Shibu, E. S.; Radha, B.; Verma, P. K.; Bhyrappa, P.; Kulkarni, G. U.; Pal, S. K.; Pradeep, T. *ACS Appl. Mater. Interfaces* **2009**, *1*, 2199. (l) Shibu, E. S.; Habeeb Muhammed, M. A.; Tsukuda, T.; Pradeep, T. *J. Phys. Chem. C* **2008**, *112*, 12168.

(2) (a) Crespo, P.; Litran, R.; Rojas, T. C.; Multigner, M.; Fuente, J. M.; Sanchez-Lopez, J. C.; Garcia, M. A.; Hernando, A.; Penades, S.; Fernandez, A. *Phys. Rev. Lett.* **2004**, *93*, 087204. (b) Zhu, M.; Aikens, C. M.; Hendrich, M. P.; Gupta, R.; Qian, H.; Schatz, G. C.; Jin, R. *J. Am. Chem. Soc.* **2009**, *131*, 2490.

(3) (a) Haruta, M. *Nature* **2005**, *437*, 1098. (b) Zhu, Y.; Qian, H.; Drake, B. A.; Jin, R. *Angew. Chem., Int. Ed.* **2010**, *49*, 1295.

(4) (a) Gobin, A. M.; Lee, M. H.; Halas, N. J.; James, W. D.; Drezek, R. A.; West, J. L. *Nano Lett.* **2007**, *7*, 1929. (b) Verma, A.; Uzun, O.; Hu, Y. H.; Hu, Y.; Han, H. S.; Watson, N.; Chen, S. L.; Irvine, D. J.; Stellacci, F. *Nat. Mater.* **2008**, *7*, 588.

(5) Sivaramakrishnan, S.; Chia, P. J.; Yeo, Y. C.; Chua, L. L.; Ho, P. K. H. *Nat. Mater.* **2007**, *6*, 149.

(6) Haynes, C. L.; McFarland, A. D.; Zhao, L. L.; Van Duyne, R. P.; Schatz, G. C.; Gunnarsson, L.; Prikulis, J.; Kasemo, B.; Kall, M. *J. Phys. Chem. B* **2003**, *107*, 7337.
(7) (a) Petty, J. T.; Zheng, J.; Hud, N. V.; Dickson, R. M. *J. Am. Chem. Soc.* **2004**, *126*, 5207. (b) Shen, Z.; Duan, H.; Frey, H. *Adv. Mater.* **2007**, *19*, 349. (c) Ledo-Surez, A.; Rivas, J.; Rodrguez-Abreu, C. F.; Rodrguez, M. J.; Pastor, E.; Hernandez-Creus, A.; Oseroff, S. B.; Lopez-Quintela, M. A. *Angew. Chem., Int. Ed.* **2007**, *46*, 8823. (d) Shang, L.; Dong, S. *Chem. Commun.* **2008**, 1088. (e) Dez, I.; Pusa, M.; Kulmala, S.; Jiang, H.; Walther, A.; Goldmann, A. S.; Muller, A. H. E.; Ikkala, O.; Ras, R. H. A. *Angew. Chem., Int. Ed.* **2009**, *48*, 2122. (f) Xu, H.; Suslick, K. S. *Adv. Mater.* **2010**, *22*, 1078. (g) Guo, W.; Yuan, J.; Dong, Q.; Wang, E. *J. Am. Chem. Soc.* **2010**, *132*, 932.
(8) (a) Branham, M. R.; Douglas, A. D.; Mills, A. J.; Tracy, J. B.; White, P. S.; Murray, R. W. *Langmuir* **2006**, *22*, 11376. (b) Bakr, O. M.; Amendola, V.; Aikens, C. M.; Wenselers, W.; Li, R.; Negro, L. D.; Schatz, G. C.; Stellacci, F. *Angew. Chem., Int. Ed.* **2009**, *48*, 5921.
(9) Wu, Z.; Lanni, E.; Chen, W.; Bier, M. E.; Ly, D.; Jin, R. *J. Am. Chem. Soc.* **2009**, *131*, 16672.
(10) (a) Nishida, N.; Yao, H.; Kimura, K. *Langmuir* **2008**, *24*, 2759. (b) Nishida, N.; Yao, H.; Ueda, T.; Sasaki, A.; Kimura, K. *Chem. Mater.* **2007**, *19*, 2831. (c) Cathcart, N.; Mistry, P.; Makra, C.; Pietrobon, B.; Coombs, N.; Niaraki, M. J.; Kitaev, V. *Langmuir* **2009**, *25*, 5840. (d) Rao, T. U. B.; Pradeep, T. *Angew. Chem. Int. Ed.* **2010**, *49*, 3925. (e) Yao, H.; Saeki, M.; Kimura, K. *J. Phys. Chem. C* **2010**, *114*, 15909. (f) Mrudula, K. V.; Rao, T. U. B.; Pradeep, T. *J. Mater. Chem.* **2009**, *19*, 4335. (g) Cathcart, N.; Kitaev, V. *J. Phys. Chem. C* **2010**, *114*, 16010.
(11) Hakkinen, H. *Chem. Soc. Rev.* **2008**, *37*, 1847, and references cited therein.
(12) Negishi, Y.; Chaki, N. K.; Shichibu, Y.; Whetten, R. L.; Tsukuda, T. *J. Am. Chem. Soc.* **2007**, *129*, 11322.

JA105495N